Separation Science and Technology
Publication details, including instructions for authors and subscription information:
http://www.informaworld.com/smpp/title~content=t713708471

Mass Transfer Model of Chromium Reduction in a Fluidized Bed Electrochemical Reactor

X. Hu[a]; R. G. Bautista[b]
[a] INSTITUTE OF NUCLEAR ENERGY TECHNOLOGY, TSINGHUA UNIVERSITY, BEIJING, PEOPLE'S REPUBLIC OF CHINA [b] DEPARTMENT OF CHEMICAL & METALLURGICAL ENGINEERING MACKAY SCHOOL OF MINES, UNIVERSITY OF NEVADA-RENO, RENO, NEVADA

To cite this Article Hu, X. and Bautista, R. G.(1997) 'Mass Transfer Model of Chromium Reduction in a Fluidized Bed Electrochemical Reactor', Separation Science and Technology, 32: 10, 1769 — 1785
To link to this Article: DOI: 10.1080/01496399708000734
URL: http://dx.doi.org/10.1080/01496399708000734

SEPARATION SCIENCE AND TECHNOLOGY, 32(10), pp. 1769–1785, 1997

Mass Transfer Model of Chromium Reduction in a Fluidized Bed Electrochemical Reactor

XIEN HU
INSTITUTE OF NUCLEAR ENERGY TECHNOLOGY
TSINGHUA UNIVERSITY
BEIJING 102201, PEOPLE'S REPUBLIC OF CHINA

RENATO G. BAUTISTA
DEPARTMENT OF CHEMICAL & METALLURGICAL ENGINEERING
MACKAY SCHOOL OF MINES
UNIVERSITY OF NEVADA-RENO
RENO, NEVADA 89557

ABSTRACT

A batch recycling fluidized bed electrochemical reactor system was used to recover Cr(VI) from a very dilute solution containing 2.5 g Cr/L at pH 2. It was found that the electrowinning rate is controlled by mass transfer and that the reduction process of Cr(VI) is interrupted by the formation of $Cr(H_2O)_6^{3+}$. The $Cr_2O_7^{2-}$ and $Cr(H_2O)_6^{3+}$ concentration–time relationship can be predicted by a plug flow model. A finite difference method and a complex optimization technique were used to estimate the mass transfer coefficient. At Re_p between 10 and 30, the $Cr_2O_7^{2-}$ and $Cr(H_2O)_6^{3+}$ mass transfer coefficients lie between 1.52–3.20 $\times$ 10^{-6} and 1.17–2.50 $\times$ 10^{-6} cm/s, respectively, and increase with the Reynolds number based on the particulate cathode.

INTRODUCTION

The recovery of chromium from leaching solutions and effluents from the electrochemical industry is of interest because chromium is a strategic

metal and chromium ions, especially Cr(VI), are also an environmental pollutant.

It is known that the electrodeposition of industrial chromium is a very slow and inefficient process (1), especially for lower concentration of chromium. A fluidized bed electrochemical reactor (FBER) can improve the process because its particulate electrode has a large specific area and turbulence between metal particles and catholyte will improve the mass transfer.

Hu and Bautista (2) showed that the electrowinning of chromium from very dilute chromic acid solution is feasible using a FBER. Even though a much lower concentration of chromium than that of the usual plating bath was used, the current efficiency still reached or exceeded that of the usual plating bath (3). If the usual plain electrodes worked with the dilute catholyte, the current efficiency would be near zero (4). Hu and Bautista also observed that the color of the CrO_3—H_2SO_4 catholyte gradually changed from light orange to dark green during electrowinning. Chromium ions in aqueous solution exist in different complex ionic forms which are dependent on the total Cr(VI) concentration and the pH (5). The predominance diagram indicates that $Cr_2O_7^{2-}$ with an orange color is the predominant species of Cr(VI) for the experimental concentration range of 2.5 g Cr/L and pH 2. During electrowinning the orange $Cr_2O_7^{2-}$ was gradually reduced to the less toxic $Cr(H_2O)_6^{3+}$ ion with a dark green color.

Although many hypotheses on the mechanism of chromium electrodeposition have been presented, the problem has not yet been resolved satisfactory (4). From analysis of the steady-state polarization curve obtained on small Pt bead microcathodes in various chromates, Hoare (6) presented a chromium electrodeposition model that assumed metallic Cr not to be electrodeposited directly from Cr(III) because the Cr(III) ion partially forms an aquo complex, $Cr(H_2O)_6^{3+}$, whose inner coordination sphere is so tightly bound that the Cr(III) cannot be discharged from this complex. In addition, Ryan considered that the electrodeposition of chromium took place through products formed in the viscous cathode film and not directly from the catholyte (7). Qin and Fang confirmed the formation of the cathode film by AES and XPS techniques (8, 9). Solodkova also studied the cathode film formed during electrochemical reduction of chromic acid over a wide range of potential (10). In general, the rate of oxidation or reduction reaction is much more rapid than that of transport, so that mass transfer in or near the film would be an important factor affecting the deposition rate.

In this work the mass transfer of $Cr_2O_7^{2-}$ and $Cr(H_2O)_6^{3+}$ will be discussed in order to estimate the reduction rate of chromium and to give some insight to the design and operation of a FBER.

MODEL DEVELOPMENT

Based on Hoare's results as reported above, it is reasonable to assume that the reduction of Cr(VI) to Cr(0) takes place stepwise and that a fraction of the intermediate Cr(III) species forms $Cr(H_2O)_6^{3+}$. The expected reactions occurring in the electrowinning of chromium are listed in Table 1.

The electrowinning of chromium on the surface of a particulate chromium cathode is supposed to occur by the following steps:

1. Transport of the chromium ion, $Cr_2O_7^{2-}$, from the bulk solution to the cathode surface.
2. Reduction of $Cr_2O_7^{2-}$ to Cr(III), with the reduction of non-aquo complexed Cr(III) to Cr(0), and all the reductions to be carried out instantaneously.
3. Transport of the aquo complex reduction reaction product, $Cr(H_2O)_6^{3+}$, from the cathode surface back to the bulk solution.

For a batch recirculating fluidized bed electrochemical reactor system the following assumptions were made in modeling the $Cr_2O_7^{2-}$ and $Cr(H_2O)_6^{3+}$ concentration–time relationship during electrowinning:

1. The rate of reduction and deposition is dependent on the rate of transport of chromium ions.
2. The FBER is operated under the condition of limiting current density for $Cr_2O_7^{2-}$, i.e., the $Cr_2O_7^{2-}$ concentration on the surface of the particulate cathode is zero.
3. Both the catholyte and the anolyte are perfectly mixed in their individual reservoirs.

TABLE 1
The Main Reactions in Electrowinning of Chromium (reaction between lead and H_2SO_4 in anolyte is not shown)

At chromium powder cathode:	
$Cr_2O_7^{2-} + 14H^+ + 6e \Leftrightarrow 2Cr^{3+} + 7H_2O$	$E_0 = 1.33$ V
$Cr^{3+} + 6H_2O \Leftrightarrow Cr(H_2O)_6^{3+}$	
$Cr^{3+} + e \Leftrightarrow Cr^{2+}$	$E_0 = -0.41$ V
$Cr^{2+} + 2e \Leftrightarrow Cr$	$E_0 = -0.91$ V
$2H^+ + 2e \Leftrightarrow H_2(g)$	$E_0 = 0$
At lead anode:	
$2Cr^{3+} + 7H_2O \Leftrightarrow Cr_2O_7^{2-} + 14H^+ + 6e$	$E_0 = -1.33$ V
$2H_2O \Leftrightarrow 4H^+ + O_2(g) + 4e$	$E_0 = 1.23$ V

4. For the catholyte, idealized plug flow exists in the FBER and axial dispersion is negligible, and the particles of the cathode are perfectly mixed (11).

Mass Transfer of $Cr_2O_7^{2-}$

As shown in Fig. 1, the $Cr_2O_7^{2-}$ concentration will change with axial distance x and time t during batch recirculation operation. An element of the reactor with length δx is taken for a differential material balance. The mass flow of $Cr_2O_7^{2-}$ into the element at the plane x with volumetric flow rate Q is $QC_6(x, t)$, and the mass flow out of the plane $x + \delta x$ is

$$QC_6(x + \delta x, t) = QC_6(x, t) + Q\frac{\partial C_6(x, t)}{\partial x}\delta x \tag{1}$$

The mass transfer in the element is $k_6(A\delta x)aC_6(x, t)$, where k_6 is the mass transfer coefficient, A is the cross-sectional area of the bed, and a is the specific surface of the particulate cathode. The following equation is derived from a material balance on the element over a time interval dt with ϵ as the bed voidage:

$$\epsilon A\frac{\partial C_6(x, t)}{\partial t} = -Q\frac{\partial C_6(x, t)}{\partial x} - k_6AaC_6(x, t) \tag{2}$$

A material balance of the catholyte reservoir with a working volume V gives

$$V\frac{dC_{6,\text{in}}}{dt} = Q(C_{6,\text{out}} - C_{6,\text{in}}) \tag{3}$$

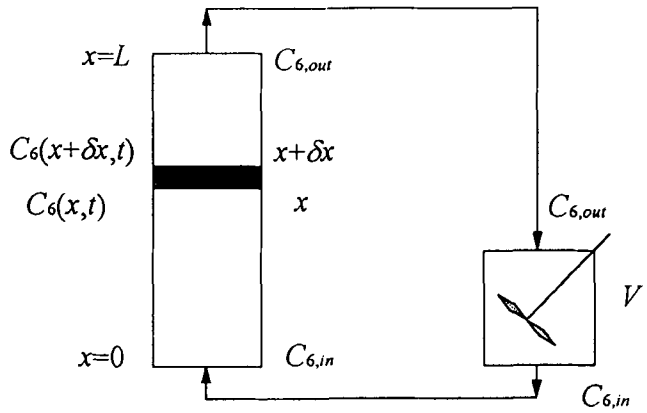

FIG. 1 Batch recirculation mode for the liquid fluidized bed electrochemical reactor.

For the convenience of data processing by computer, Eq. (2) is transformed into a finite difference equation with implicit difference schemes and constant stability:

$$\frac{C_6(x, t + \Delta t) - C_6(x, t)}{\Delta t} = -\frac{Q}{\epsilon A}\frac{C_6(x + \Delta x, t + \Delta t) - C_6(x - \Delta x, t + \Delta t)}{2\Delta x} - \frac{k_6 a}{\epsilon} C_6(x, t + \Delta t) \tag{4}$$

Equation (4) is rearranged to give

$$\frac{Q}{2\epsilon A \Delta x} C_{6,i-1,j+1} + \left(\frac{1}{\Delta t} + \frac{k_6 a}{\epsilon}\right) C_{6,i,j+1} + \frac{Q}{2\epsilon A \Delta x} C_{6,i+1,j+1} = \frac{1}{\Delta t} C_{6,i,j} \tag{5}$$

where the subscripts i and j represents distance and time, respectively.

The initial condition at $t = 0$ is

$$C_6(x, 0) = C_6^0 \tag{6}$$

where C_6^0 is the initial concentration of $Cr_2O_7^{2-}$ before switch-on, and the boundary conditions $C_6(0, t)$ and $C_6(L, t)$ should satisfy the solution of Eq. (3):

$$C_{6,0,j+1} = C_{6,l,j} - (C_{6,l,j} - C_{6,0,j}) \exp\left(-\frac{Q}{V}\Delta t\right) \tag{7}$$

and boundary condition

$$\left.\frac{\partial C_6(x, t)}{\partial x}\right|_{x=L} = 0 \tag{8}$$

where $l = L/\Delta x$. The $Cr_2O_7^{2-}$ concentration at any time $j\Delta t$ and any position $i\Delta x$ can be calculated in steps from Eqs. (5)–(8).

Mass Transfer of $Cr(H_2O)_6^{3+}$

The $Cr(H_2O)_6^{3+}$ concentration of the catholyte increases with time during electrowinning. The process can be described by transport of $Cr(H_2O)_6^{3+}$ produced by the reduction of $Cr_2O_7^{2-}$ at the particulate cathode surface to the bulk solution.

The surface concentration of $Cr(H_2O)_6^{3+}$ is not zero and the mass transfer term is $k_3(A\delta x)a[(C_{3s}(x, t) - C_3(x, t)]$. Following the procedures

used in treating $Cr_2O_7^{2-}$, the equation of mass transfer for $Cr(H_2O)_6^{3+}$ can be written as

$$\epsilon A\frac{\partial C_3(x, t)}{\partial t} = -Q\frac{\partial C_3(x, t)}{\partial x} - k_3Aa[C_{3s}(x, t) - C_3(x, t)] \quad (9)$$

and

$$V\frac{dC_{3,\text{in}}}{dt} = Q(C_{3,\text{out}} - C_{3,\text{in}}) \quad (10)$$

Equation (9) can be transformed to a finite central difference equation in the form as stated above:

$$\begin{aligned}\frac{C_3(x, t + \Delta t) - C_3(x, t)}{\Delta t} &= -\frac{Q}{\epsilon A}\frac{C_3(x + \Delta x, t + \Delta t) - C_3(x - \Delta x, t + \Delta t)}{2\Delta x} \\ &\quad + \frac{k_3a}{\epsilon}[C_{3s}(x, t + \Delta t) - C_3(x, t + \Delta t)]\end{aligned} \quad (11)$$

Equation (11) is rearranged to give

$$-\frac{Q}{2\epsilon A\Delta x}C_{3,i-1,j+1} + \left(\frac{1}{\Delta t} + \frac{k_3a}{\epsilon}\right)C_{3,i,j+1} + \frac{Q}{2\epsilon A\Delta x}C_{3,i+1,j+1} = \frac{1}{\Delta t}C_{3,i,j} + \frac{k_3a}{\epsilon}C_{3s,i,j+1} \quad (12)$$

The initial condition is

$$C_3(x, 0) = 0 \quad (13)$$

and the boundary condition is

$$C_{3,0,j+1} = C_{3,l,j} - (C_{3,l,j} - C_{3,0,j})\exp\left(-\frac{Q}{V}\Delta t\right) \quad (14)$$

and

$$\left.\frac{\partial C_3(x, t)}{\partial x}\right|_{x=L} = 0 \quad (15)$$

In Eq. (9) the surface concentration C_{3s} is unknown. In order to estimate C_{3s}, the concentration distribution around the cathode should be analyzed.

Figure 2 shows the concentration profile adjacent to the particulate cathode surface r with the distance from the surface. The $Cr_2O_7^{2-}$ concentration decreases to zero at the plane $r = 0$ as $Cr_2O_7^{2-}$ is reduced under

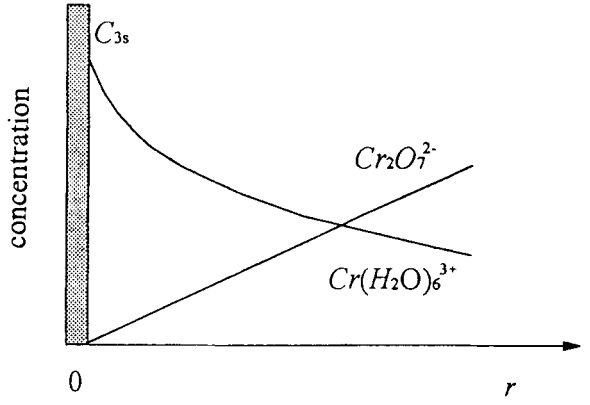

FIG. 2 The chromium concentration profile near the particular cathode surface.

the limiting current. The $Cr(H_2O)_6^{3+}$ concentration decreases along the direction r with a concentration gradient dependent on the transport resistance. Taking into account the short bed used in this work and the perfectly mixed cathode particles in the model for simplicity, the axial distribution of the $Cr(H_2O)_6^{3+}$ concentration on the cathode surface could be considered to be constant, i.e.,

$$C_{3s}(x, t) = C_{3s}(t) \tag{16}$$

In other words, the value of $C_{3s}(t)$ could also be taken as the mean value along the bed length. A material balance is made at a volume element close to the surface with thickness dr and cross-sectional area S. The conversion ratio is defined by

$$\zeta = \Delta m_3/\Delta m_6 \tag{17}$$

where Δm_6 is the mass of $Cr_2O_7^{2-}$ disappearing during the reduction, and Δm_3 is the yield of $Cr(H_2O)_6^{3+}$. The $Cr(H_2O)_6^{3+}$ mass flowing in the element in time dt is $Sk_6(\partial C_6/\partial r)\, drdt$, the $Cr(H_2O)_6^{3+}$ mass produced is $Sk_6\zeta(\partial C_6/\partial r)\, drdt$, and the $Cr(H_2O)_6^{3+}$ mass flowing out by transport is $-Sk_3(\partial C_3/\partial r)\, drdt$. The mass change of $Cr(H_2O)_6^{3+}$ in the element is

$$(Sdr)dC_{3s} = Sk_6\zeta\left(\frac{\partial C_6}{\partial r}\right)drdt + Sk_3\left(\frac{\partial C_3}{\partial r}\right)drdt \tag{18}$$

Equation (18) can be reduced to

$$\frac{dC_{3s}}{dt} = k_6\zeta\left(\frac{\partial C_6}{\partial r}\right) + k_3\left(\frac{\partial C_3}{\partial r}\right) \tag{19}$$

As an approximation, $\partial C_6/\partial r$, the concentration gradient of $Cr_2O_7^{2-}$, can be assumed to be a constant, λ, during the operation. Based on the Nerst equation,

$$\left(\frac{\partial C_3}{\partial r}\right)_{r=0} = -\frac{i_3}{ZFD} \tag{20}$$

The current density i_3 is the contribution of Cr(III) ion to be reduced to the total current density. Because the conversion and current efficiency of reduction could be taken as constant, i_3 is proportional to the cell current $I(t)$, i.e.,

$$i_3 = \psi I(t) \tag{21}$$

Then

$$\left(\frac{\partial C_3}{\partial r}\right)_{r=0} = -\frac{\psi}{ZFD}I(t) \tag{22}$$

Substituting Eq. (22) into Eq. (19) results in

$$\frac{dC_3}{dr} = k_6\zeta\lambda - k_3\frac{\psi}{ZFD}I(t) \tag{23}$$

With the function $I(t)$ determined experimentally, $C_{3s}(t)$ can be obtained by solving Eq. (23).

EXPERIMENTAL

Materials

Deionized water and reagent grade H_2SO_4 and CrO_3 were used in this work. H_2SO_4 was added dropwise to deionized water until the pH was 2, then weighted CrO_3 was dissolved in the pH 2 sulfuric acid solution to prepare catholyte of the desired concentration. The adjusted pH 2 sulfuric acid solution was also used for anolyte. The -20 mesh chromium particles (Thiokol Co.) were ground and sieved, and powder in the range of 450–600 μm was used as the particulate cathode.

Apparatus

The FBER was constructed from a Plexiglas cylinder 35.6 cm long with 8.9 cm O.D. and 7.6 cm I.D. The anode was located inside the cylindrical diaphragm in the center of the bed. It was made of a lead tube 1.6 cm in diameter, attached to copper tube which served as the inlet for the anolyte. The membrane between the anode and the cathode was a porous Vycor glass tube, selective to hydrogen ion, made by Corning Glass. The ion selectivity helped lower the resistance in the cell circuitry. Six carbon bars in the cathode chamber served as the current feeder, and they projected into the center of the bed.

Procedures

The experiments were carried out at constant cell voltage, known initial chromium concentration, and at different volumetric flow rates. The experimental conditions are listed in Table 2.

The concentrations of $Cr_2O_7^{2-}$ and $Cr(H_2O)_6^{3+}$ in the catholyte reservoir were determined by a colorimetric method (12). The species $Cr_2O_7^{2-}$ and $Cr(H_2O)_6^{3+}$ were simultaneously determined based on their individual color. The solution was maintained at an appropriate acidity to prevent the formation of polynuclear complexes of Cr(III). At 1 M H_2SO_4 the absorbance for $Cr_2O_7^{2-}$ could be read at 500 nm and that of $Cr(H_2O)_6^{3+}$ at 590 nm. The absorbance of $Cr_2O_7^{2-}$ or $Cr(H_2O)_6^{3+}$ was found to be proportional to the concentration without mutual interference. The calibration curves for both species are shown in Fig. 3.

TABLE 2
Summary of Experimental Conditions

Fluidized bed:	
Cross-section area	30.0 cm^2
Specific surface of particulate cathode	52.0 cm^2/cm^3
Bed expansion	0.15–0.35
Catholyte:	
CrO_3-H_2SO_4	2.5 g Cr/L, pH 2
Anolyte:	
H_2SO_4	pH 2
Catholyte reservoir volume	1400 cm^3
Cell voltage	10.0 V
Temperature	21–23°C
Operating time for each run	5 hours

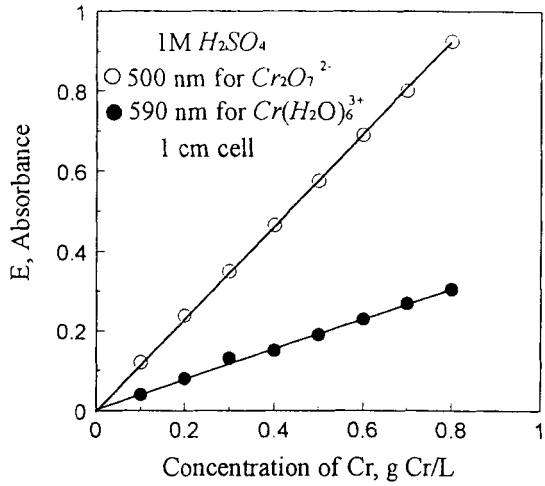

FIG. 3 The calibration curve for chromium.

RESULTS AND DISCUSSION

Mass Transfer of $Cr_2O_7^{2-}$

In Eq. (4) only one parameter, the mass transfer coefficient k_6, is unknown. If the value of k_6 is assumed, the $Cr_2O_7^{2-}$ concentration–time relationship can be obtained by solving Eq. (5) with relevant initial and boundary conditions. The mass transfer coefficient of $Cr_2O_7^{2-}$ was estimated by the least-squares fitting between the calculated and experimental concentration of $Cr_2O_7^{2-}$ in the catholyte reservoir. A trial-and-error search method (Golden Section One Dimension Search Program) was used. The objective function is

$$J = \sum_{p=1}^{q} (C_{6,i,\text{calc}} - C_{6,i,\text{expt}})_p^2 \tag{24}$$

where q is the total number of experimental data. The value of k_6 can be obtained by minimizing the objective function.

The model and mass transfer coefficient k_6 were used to predict the $Cr_2O_7^{2-}$ concentration–time relationship. In Fig. 4, four sets of experimental data of $Cr_2O_7^{2-}$ concentration at different times were compared with the predicted model values. The mean relative error was found to be 1.27%. A typical plot of the $Cr_2O_7^{2-}$ concentration–time relationship is shown in Fig. 5.

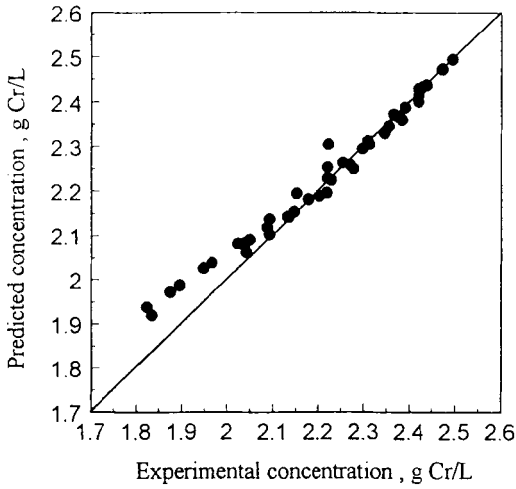

FIG. 4 The predicted concentration versus the experimental concentration for $Cr_2O_7^{2-}$.

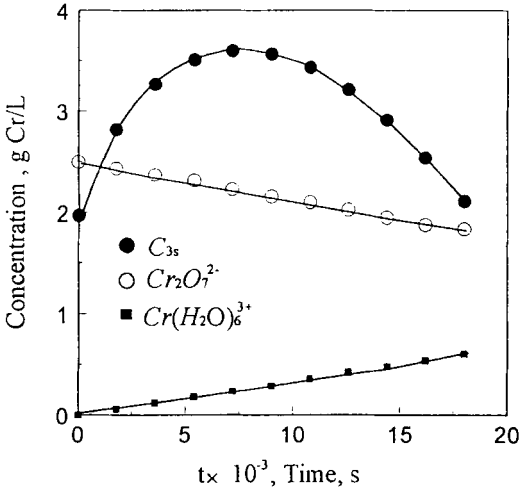

FIG. 5 Plot of $Cr_2O_7^{2-}$, $Cr(H_2O)_6^{3+}$, and C_{3s} versus the time at $Re_p = 27.8$.

Mass Transfer of $Cr(H_2O)_6^{3+}$

The correlation of the cathode surface concentration of Cr(III) with time is given by Eq. (23). The conversion ratio, ξ, and the relation of the cell current to time, $I(t)$, can be determined experimentally.

The conversion ratio, ξ, was calculated in terms of the mass disappearance of Cr(VI), Δm_6, and the yield of Cr(III), Δm_3, at different times for a run. The plot of Δm_3 versus Δm_6 for the run at $Re_p = 27.8$ is shown in Fig. 6. The value of ξ can be determined from the slope of the straight line. The relationship of cell current to time can be represented by an empirical equation in the form of a polynomial:

$$I(t) = \theta_1 t^{\theta_2} + \theta_3 \tag{25}$$

It was found experimentally that a steep step current occurs in the cell circuit. Therefore the constant θ_3 should be the current at $t = 0^+$. The other constants, θ_1 and θ_2, can be obtained by linear regression. A log-log plot of $I(t) - \theta_3$ versus time is shown in Fig. 7 for the run at $Re_p = 20.0$ and $\theta_2 = 0.1383$. The correlation coefficient R was found to be 0.9660.

Substituting Eq. (25) into Eq. (23) and rearranging gives

$$\frac{dC_{3s}(t)}{dt} = k_6\zeta\lambda - \left(\frac{\psi k_3}{ZFD}\right)\theta_3 - \left(\frac{\psi k_3\theta_1}{ZFD}\right)t^{\theta_2} \tag{26}$$

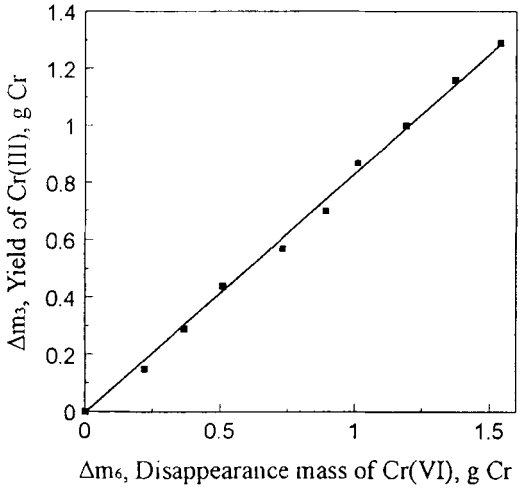

FIG. 6 The relation of Cr(III) yield to the disappearance mass of Cr(VI) at $Re_p = 27.8$.

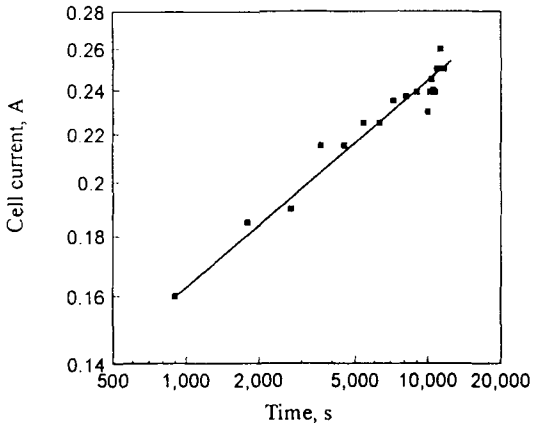

FIG. 7 Plot of cell current versus time at $Re_p = 19.9$.

Integrate Eq. (26) over time t and let

$$a_1 = k_6\zeta\lambda - \left(\frac{\psi k_3}{ZFD}\right)\theta_3 \tag{27}$$

$$a_2 = \left(\frac{\psi k_3}{ZFD}\right)\frac{\theta_1}{\theta_2 + 1} \tag{28}$$

The surface concentration of $Cr(H_2O)_6^{3+}$ as a function of time is given by

$$C_{3s}(t) = a_1 t + a_2 t^{\theta_2 + 1} + C_{3s}^0 \tag{29}$$

By considering the step current response at the moment of switch-on, C_{3s}^0 would be equal to the concentration converted from C_6^0 by a factor of ζ, i.e.,

$$C_{3s}^0 = C_6^0 \tag{30}$$

The $Cr(H_2O)_6^{3+}$ concentration–time relationship could be solved by combining Eqs. (13)–(15) and (29). The three unknown parameters, a_1, a_2, and k_3, in these equations can be estimated by the least-squares fitting method similar to the procedure used in estimating k_6. An optimum complex program was used to search for a set of a_1, a_2, and k_3 to minimize the error between predicted and experimental data. For example, $a_1 = 1.0606 \times 10^{-6}$, $a_2 = 8.3202 \times 10^{-8}$ (for concentration in g/cm^3 and time in seconds), and $k_3 = 2.50 \times 10^{-6}$ cm/s were obtained for the run at Re_p

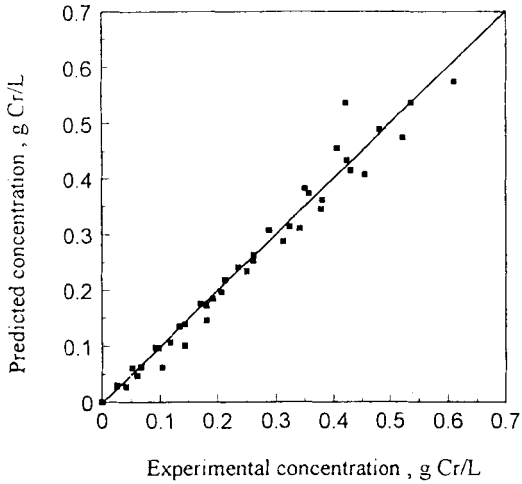

FIG. 8 The predicted concentration versus the experimental concentration for $Cr(H_2O)_6^{3+}$.

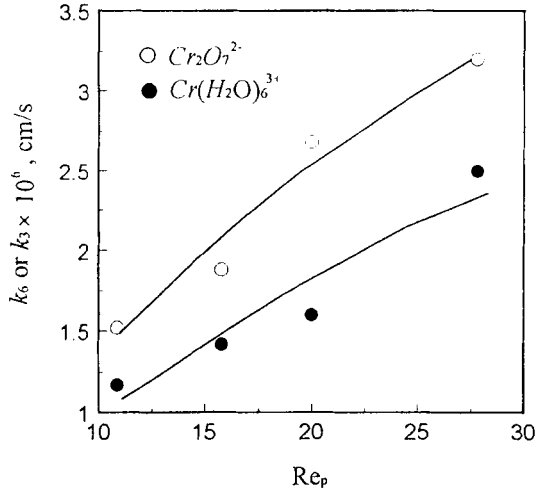

FIG. 9 Plot of mass transfer coefficient versus particulate Reynolds number.

= 27.8. $Cr_2O_7^{2-}$, $Cr(H_2O)_6^{3+}$, and C_{3s}–time relationships are shown in Fig. 5 for this run. The model was used to predict the $Cr(H_2O)_6^{3+}$ concentration–time relationship during electrowinning. Four sets of predicted data are compared with experimental values in Fig. 8; the mean relative error was 8.3%.

The mass transfer coefficients, k_6 and k_3, based on the above model are plotted versus the Reynolds number of the particulated cathode in Fig. 9. It was found that the mass transfer coefficients increased with Re_p in the experimental range. These results confirm that the electrowinning rate was controlled by mass transfer.

CONCLUSIONS

A very dilute concentration of chromic acid (about 2.5 g Cr/L and pH 2) was used as the catholyte in the electrowinning of chromium in a FBER. The results show that hexavalent chromium cannot entirely be reduced to metal, and a fraction of the intermediate Cr(III) forms a stable $Cr(H_2O)_6^{3+}$ ion. Cr(III) is less toxic environmentally than Cr(VI).

It was also found that the electrowinning rate was controlled by mass transfer of $Cr_2O_7^{2-}$ and $Cr(H_2O)_6^{3+}$. An idealized plug flow model was found to be in good agreement with the experimental data for a batch recirculating system. The $Cr_2O_7^{2-}$ and $Cr(H_2O)_6^{3+}$ mass transfer coefficients can be estimated by an optimum complex technique to minimize the error between the predicted and experimental values. At Re_p between 10 and 30, the $Cr_2O_7^{2-}$ and $Cr(H_2O)_6^{3+}$ mass transfer coefficients lie between $1.52–3.20 \times 10^{-6}$ and $1.17–2.50 \times 10^{-6}$ cm/s, respectively, and increase with increasing Reynolds number based on the particulated cathode.

NOMENCLATURE

A	cross-section area of bed (cm^2)
a	specific surface of particulate cathode (cm^2/cm^3)
a_1, a_2	constant in Eqs. (27) and (28)
C	concentration (g Cr/L)
D	diffusivity (cm^2/s)
E	absorbance in spectrophotometry
F	Faraday constant
I	cell current (A)
i	current density (A/cm^2)
J	objective function
k	mass transfer coefficient (cm/s)

L	length of bed (cm)
p	number of experimental value
Q	volumetric flow rate (cm^3/s)
q	total number of experimental value
r	distance (cm)
S	cross-section area of element (cm^2)
t	time (s)
V	volume of catholyte reservoir (cm^3)
x	distance (cm)
Z	valence

Greek Symbols

ϵ	bed voidage
ζ	conversion ratio
$\theta_1, \theta_2, \theta_3$	constants in Eq. (25)
λ	constant in Eq. (23)
ψ	constant in Eq. (21)

Subscripts

calc	calculated
expt	experimental
i	distance of the element
in	inlet of bed
j	time for the element
l	represents the element at $x = L$
out	outlet of bed
s	surface
3	$Cr(H_2O)_6^{3+}$
6	$Cr_2O_7^{2-}$

Superscript

0	initial

REFERENCES

1. J. P. Hoare, A. H. Holden, and M. A. Laboda, *Plat. Surf. Finish.*, *67*, 42 (1980).
2. X. Hu and R. G. Bautista, *Sep. Sci. Technol.*, *23*, 1989 (1988).
3. O. D. Pletcher, *Industrial Electrochemistry*, Chapman and Hall Ltd., New York, NY, 1982, p. 186.
4. D. T. Chin and H. Zhang, *Electrochim. Acta.*, *31*, 299 (1986).
5. A. K. Sengupta and D. Clifford, *Ind. Eng. Chem., Fundam.*, *25*, 249 (1986).

6. J. P. Hoare, *J. Electrochem. Soc.*, *126*, 190 (1979).
7. N. E. Ryan, *ARL Met. Rep.*, *53* (1964).
8. Q. Qin, S. Liu, D. Cheng, et al., *Acta Physico-Chim. Sinica*, *8*, 571 (1992).
9. J. L. Fang, N. J. Wu, and Z. W. Wang, *J. Appl. Electrochem.*, *23*, 495 (1993).
10. L. N. Solodkova and Z. A. Solov'eva, *Elektrokhimiya*, *30*, 1254 (1994).
11. A. T. S. Walker and A. A. Wragg, *Electrochim. Acta*, *22*, 1129 (1977).
12. M. J. Cardone and J. Compton, *Anal. Chem.*, *24*, 1903 (1952).

Received by editor March 7, 1996
Revision received November 12, 1996